

Study Thermal Property of Stereolithography 3D Printed
Multiwalled Carbon Nanotubes Filled Polymer Nanocomposite

by

Kunal Manoj Gide

A Thesis Presented in Partial Fulfillment
of the Requirements for the Degree
Master of Science

Approved November 2020 by the
Graduate Supervisory Committee:

Qiong Nian, Chair
Beomjin Kwon
Xiangjia Li

ARIZONA STATE UNIVERSITY

December 2020

ABSTRACT

Traditionally, for applications that require heat transfer (e.g. heat exchangers), metals have been the go-to material for manufacturers because of their high thermal as well as structural properties. However, metals have some notable drawbacks. They are not corrosion-resistant, offer no freedom of design, have a high cost of production, and sourcing the material itself. Even though polymers on their own don't show great prospects in the field of thermal applications, their composites perform better than their counterparts. Nanofillers, when added to a polymer matrix not only increase their structural strength but also their thermal performance. This work aims to tackle two of those problems by using the additive manufacturing method, stereolithography to solve the problem of design freedom, and the use of polymer nanocomposite material for corrosion-resistance and increase their overall thermal performance. In this work, three different concentrations of polymer composite materials were studied: 0.25 wt%, 0.5 wt%, and 1wt% for their thermal conductivity. The samples were prepared by magnetically stirring them for a period of 10 to 24 hours depending on their concentrations and then sonicating in an ice bath further for a period of 2 to 3 hours. These samples were then tested for their thermal conductivities using a Hot Disk TPS 2500S. Scanning Electron Microscope (SEM) to study the dispersion of the nanoparticles in the matrix. Different theoretical models were studied and used to compare experimental data to the predicted values of effective thermal conductivity. An increase of 7.9 % in thermal conductivity of the composite material was recorded for just 1 wt% addition of multiwalled carbon nanotubes (MWCNTs).

DEDICATION

This thesis work is dedicated to my parents, Manoj and Asha Gide, who have been a constant source of support and encouragement during the challenges of graduate school and life. This work is also dedicated to Sarika, my sister Manali, and brother-in-law Rohan Kanavje, who have always believed in me and persistently reminded me of my goals and dreams. I would like to thank my brother, Milind Gide, who has helped me throughout this journey with his guidance. Lastly, I would like to dedicate this work to my family and friends, who have always been with me and helped me grow into the person I am today.

ACKNOWLEDGMENTS

At the very outset of this report, I would like to extend my sincere and heartfelt obligation towards all the people who have helped me in this endeavor. Without their guidance, help, encouragement, and cooperation, I would not have made headway in this thesis.

I am indebted to Dr. Qiong Nian (Committee Chair) for conscientious guidance and encouragement to accomplish this work. I could not have imagined a better advisor and mentor for my thesis study.

I am extremely thankful and pay my gratitude to my committee members, Dr. Beomjin Kwon and Dr. Xiangjia Li, for their valuable guidance and support for the completion of this thesis.

I extend my gratitude to Arizona State University for giving me this opportunity.

I would again like to thank Dr. Beomjin Kwon for his continued support of my lab equipment access. Also, my sincere acknowledgment goes to Rui Dai for his help in conducting thermal tests, taking SEM images, and his overall contribution with insightful comments and discussion regarding the work.

I also acknowledge with a deep sense of reverence, my gratitude towards my parents, and members of my family, who have always supported me morally as well as economically.

At last but not least gratitude goes to all of my friends who directly or indirectly helped me complete this thesis.

TABLE OF CONTENTS

	Page
LIST OF TABLES	vi
LIST OF FIGURES	vii
LIST OF SYMBOLS / NOMENCLATURE.....	viii
CHAPTER	
1 INTRODUCTION	1
1.1 Polymers	1
1.2 Carbon-based Nanoparticles	4
1.2.1 Nanodiamonds	4
1.2.2 Fullerene	5
1.2.3 Graphite	7
1.2.4 Graphene Nanoplatelets	8
1.2.5 Carbon Nanotubes	9
1.3 Additive Manufacturing Processes	12
1.3.1 Fused Deposition Modeling.....	13
1.3.2 Selective Laser Sintering	14
1.3.3 Stereolithography	17
2 MATERIALS AND EXPERIMENTAL SETUP.....	19
2.1 Materials	19
2.1.1 Resin	19
2.1.2 Carbon Nanotubes	20
2.1.3 Titan 2	20

CHAPTER	Page
2.2 Nanocomposite Preparation	21
2.3 CAD Model and Parameter for 3D Printing.....	22
2.4 TPS 2500S	25
3 RESULTS AND DISCUSSION.....	28
3.1 Dispersion of Filler Material	28
3.2 Measurement of Thermal Conductivity with TPS 2500S	29
3.3 Understanding Thermal Conductivity Enhancement using Different Models.....	31
4 CONCLUSION	37
5 FUTURE SCOPE	38
5.1 Higher Filler Concentration	38
5.2 Use of Different Material	38
5.3 Surface Modification of Filler Material.....	39
5.4 Incorporating in Thermal Application.....	39
REFERENCES	40

LIST OF TABLES

Table		Page
1.	Some Common Types of Polymers	2
2.	Thermal Conductivity of Some Common Polymers at Room Temperature	3
3.	Parameters for Printing Sample with Pure Resin	23
4.	Parameters for Printing Sample with 0.25 wt% of MWCNT	23
5.	Parameters for Printing Sample with 0.5 wt% of MWCNT	24
6.	Parameters for Printing Sample with 1 wt% of MWCNT	24

LIST OF FIGURES

Figure	Page
1. Nanodiamonds.....	4
2. Fullerene	5
3. Graphite	7
4. Graphene Nanoplatelets (GnP)	8
5. Carbon Nanotubes (CNTs).....	9
6. Schematic Representation of CNT Formation	10
7. Fused Deposition Modeling (FDM)	13
8. Selective Laser Sintering (SLS).....	15
9. Stereolithography (SLA).....	17
10. Resin in a bottle and a Beaker.....	19
11. TEM image of MWCNT.....	20
12. Setup for SLA 3D Printing.....	21
13. Machines Used for Homogenous Mixing of Samples.....	22
14. Schematic of TPS 2500S Test Arrangement.....	26
15. Test Arrangement for TPS 2500S.....	27
16. SEM Images of CNT Composites.....	28
17. SEM images of CNT Composites.....	29
18. Experimental Reading of Thermal Conductivity.....	30
19. Experimental Values of Thermal Conductivity.....	30
20. Comparison of Experimental Results with Theoretical Models.....	34

LIST OF SYMBOLS

Symbol

1. ND Nanodiamonds
2. GnPGraphene Nanoplatelets
3. CNTCarbon Nanotubes
4. SWCNTSingle-walled Carbon Nanotubes
5. MWCNTMulti-walled Carbon Nanotubes
6. IPAIsopropyl Alcohol
7. CVDChemical Vapor Deposition
8. DNDDetonation Synthesis
9. AMAdditive Manufacturing Processes
10. FDMFused Deposition Modeling
11. SLSSelective Laser Sintering
12. SLAStereolithography
13. SEMScanning Electron Microscope

CHAPTER 1

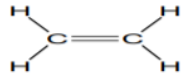
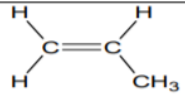
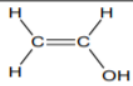
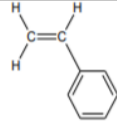
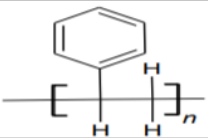
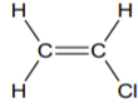
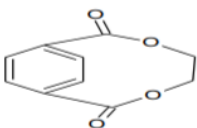
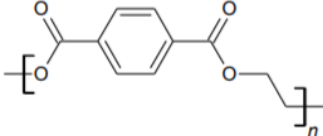
INTRODUCTION

This chapter contains a brief overview of different types of polymers, carbon-based nanoparticles, and some common additive manufacturing techniques. It discusses the history, properties, advantages, and disadvantages of each along with their applications.

1.1 Polymers

(Verma et al., 2018)Polymers occur in both natural and synthetic forms. Cotton, wool, and paper reed (used for paper) are some of the early examples of the use of polymers by humankind. John Wesley Hyatt in 1869, treated cellulose derived from cotton fiber to discover a plastic that could be mouldable and imitated natural polymers. Synthetic polymers came into existence in the early 1900s. Bakelite was invented in 1907 by Leo Baekeland using synthetic components. It has properties such as low electrical conductivity, thermal insulation, easily moldable, etc. Most of the synthetic polymers show properties similar to these. Polymers are covalently bonded chain or network of monomers. This reaction is known as polymerization reaction. Polymers had a different structure than metals, ceramics which led to them having certain advantages over them. Polymers generally weigh much lesser than metals which translates to cost reductions in many ways. They are also less susceptible to chemical attacks and are easy and faster to manufacture.

Table 1*Table for Some Common Types of Polymer.*

Some common types of polymers		
Example	Monomer	Polymer
Polyethylene		$[\text{CH}_2-\text{CH}_2-]_n$
Polypropylene		$[\text{CH}(\text{CH}_3)-\text{CH}_2-]_n$
Polyvinyl Alcohol		$[\text{CH}(\text{OH})-\text{CH}_2-]_n$
Polystyrene		
Polyvinyl Chloride		$[\text{CH}_2-\text{CH}(\text{Cl})-]_n$
Polyethylene Terephthalate		

Note. (Verma et al., 2018)

Polymers are used in various applications. They can be found in every sector. Even though polymers have many advantages over metals, they have notable limitations. The use of polymers for thermal applications can be hindered by their low thermal conductivities as shown in Table 2.

Table 2

Table for Thermal Conductivity of Some Common Polymers at Room Temperatures

Material	Thermal Conductivity (W m ⁻¹ K ⁻¹)	Density (kg m ⁻³)
Low density polyethylene (LDPE)	0.33	917-930
High density polyethylene (HDPE)	0.45-0.52	930-970
Polypropylene (PP)	0.14	946
Polyvinyl chloride (PVC)	0.12-0.17	1300-1400
Polyetheretherketone (PEEK)	0.25	1320
Epoxy	0.17-0.21	1250
Polymethyl metacrylate (PMMA)	0.15-0.25	1150-1190

Note. (Danayat et al., 2019)

The addition of filler material to polymers is one way to increase their thermal conductivities. Filler material with high thermal conductivities like carbon-based nanofillers can considerably increase the thermal conductivity of the polymer matrix.

Polymer composites have the potential to become the go-to material for thermal applications due to their unique properties and a wide range of applications.

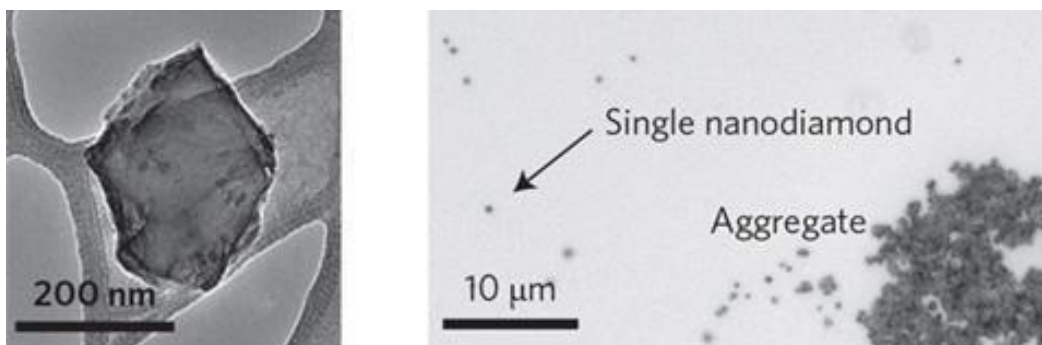
1.2 Carbon-based Nanoparticles

Typically, particles that have one of its dimensions in a range of 1-100 nm are known as nanoparticles though sometimes, they might be as large as 500 nm. Carbon-based nanoparticles have been widely used as filler materials for polymer composites. It is known to increase their electrical and thermo-mechanical properties to a significant extent. Some types of carbon-based nanoparticles are nanodiamonds, fullerene, carbon nanotubes, graphite, and graphene.

1.2.1 Nanodiamonds

Figure 1

Nanodiamonds



Note. (*Nanodiamonds Add Some Sparkle to Imaging | Research | Chemistry World*, n.d.)

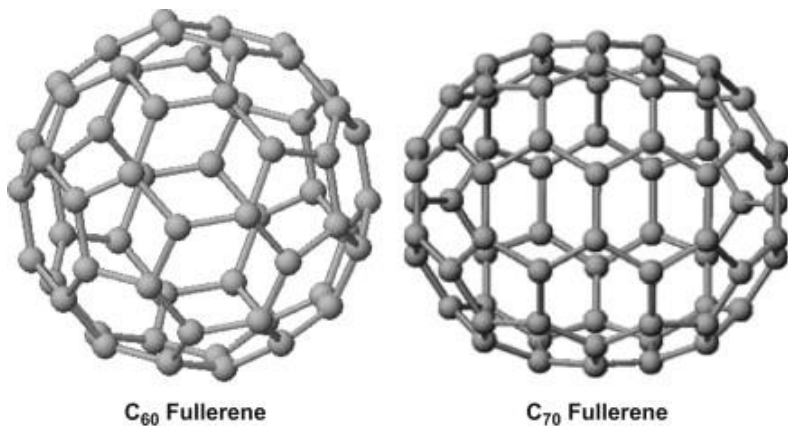
Nanodiamonds are one of the allotropes of carbon nanoparticles which have many useful characteristics like physical, mechanical, thermal, optical, and biocompatible. The structure of a nanodiamond (ND) has a diameter of 2-10 nm. They have high absorption energy, and a large surface area compared to other types of nanoparticles. (Santos & Martel, 2018) They are mainly used for biomedical applications like drug delivery and

imaging systems. Their specialized structure of an inert core and reactive shell makes them an excellent candidate to use as carriers for biomarkers, biosensors, biologically active substances, etc. ND's can be manufactured by high pressure and high temperature (HPHT), chemical vapor deposition (CVD), and detonation synthesis (DND). They are synthesized by the detonation of explosives in an oxygen-deficient atmosphere, characterized by a narrow size distribution. For HPHT manufacturing pressures of 70-80 kbar and temperatures up to 1400-1600 °C are attained. In CVD synthesis, carbon atoms are deposited on a substrate to grow diamond films after a series of reactions by ionizing a hydrocarbon gas mixture. Even though ND's are used for most of the biomedical application they are subject to toxicity tests. The degree of toxicity allowed depends on the type of applications, it has been found that concentrations of more than 50 µg/ml of unattached nanoparticles can have a toxic effect on cells as they can easily penetrate them.

1.2.2 Fullerene

Figure 2

Fullerene



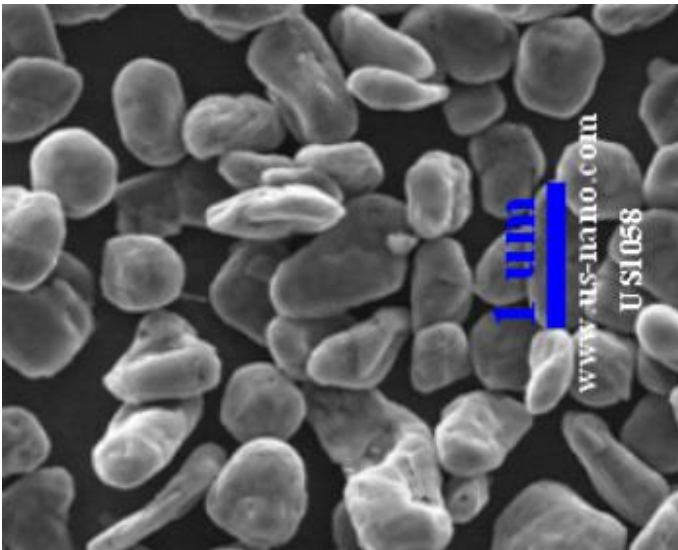
Note. (*Fullerene Nanofiller - Google Search, n.d.*)

(Penkova et al., 2017) Buckminsterfullerene or C₆₀ was discovered in 1985 by R. Smalley, R. Curl, and H. Kroto. It is the only allotrope of carbon with a fixed number of atoms. The inherent properties of fullerene have made them useful for some applications like light-activated antimicrobial agents, superconductivity, high heat resistant materials, and biocompatibility in the field of medicine. (Zuev, 2011) Fullerene, when used as nano-fillers in polymer composites, have shown to increase the polymer's physical properties at very low filler loading. Because of this, they have been used in photovoltaic cells, biomedical devices, fuel cells, and membrane processes. (Yadav, 2018) Fullerene is synthesized using the arc discharge method. In this method, a large current is passed through two carbon electrodes placed in an inert atmosphere such as helium. When the current is passed, a carbon plasma arc is formed bridging the electrodes which cool instantaneously leaving behind sooty residue from which fullerene can be extracted. The structure of fullerene is a closed cage-like structure that resembles a soccer ball that is why it is sometimes known as 'buckyball' structure as seen in Figure 2. C₆₀ fullerene is made up of 20 hexagonal and 12 pentagonal carbon structures. There are also fullerenes with C₇₀ and C₈₀ carbon atoms found. Despite its various advantages, there is a major drawback while using fullerene as a filler material. It is very difficult to homogeneously disperse fullerene in a polymer matrix or make a solution. Also, there are strong interfacial interactions to affect efficient load transfer from the polymer matrix to fullerene.

1.2.3 Graphite

Figure 3

Graphite



Note. (*Graphite Nanopowder - Google Search, n.d.*)

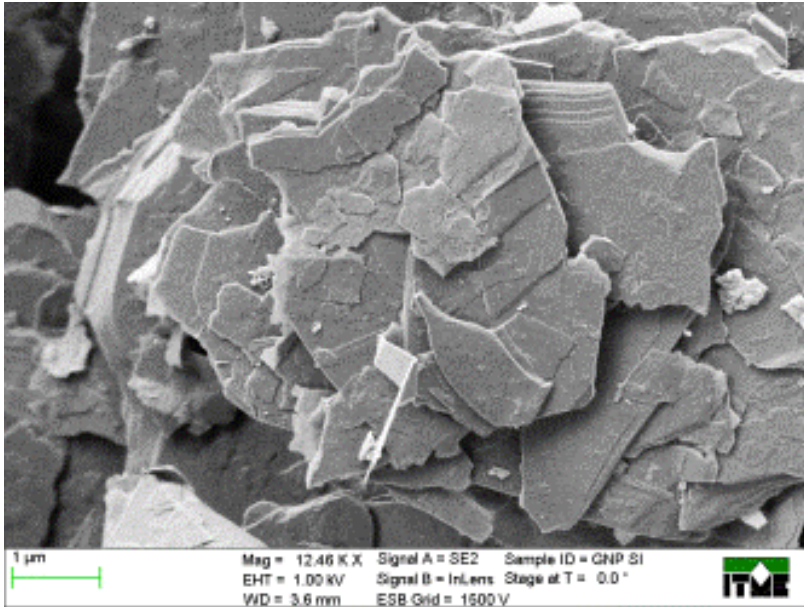
(Fukushima, 2003) Graphite is a gray crystalline allotropic form of carbon with a hexagonal structure. It occurs naturally in this form and is the most stable allotrope of carbon under normal conditions. It is found in metamorphic rocks in the continents of Asia, South America, and a few parts of North America. It is the stiffest naturally occurring material. It is known to be a good conductor of heat and electricity. Graphite nanoparticles have shown to have excellent thermal, mechanical, and electrical properties due to which they are used in a wide range of applications such as biosensors, fuel cells, transistors, and composites (nanocomposites & 2009, n.d.). It performs well under conditions exceeding 3600 °C. It is self-lubricating as well as resistant to chemical reactions. Graphite nanoparticles are used in the nuclear industry for fabrication and

lining of the nuclear plant, heat moderators, etc, and also used as a secondary shut down material due to its high thermal stability.

1.2.4 Graphene Nanoplatelets (GnP)

Figure 4

Graphene Nanoplatelets (GnP)



Note. (*Graphene Nanoplatelets - Google Search, n.d.*)

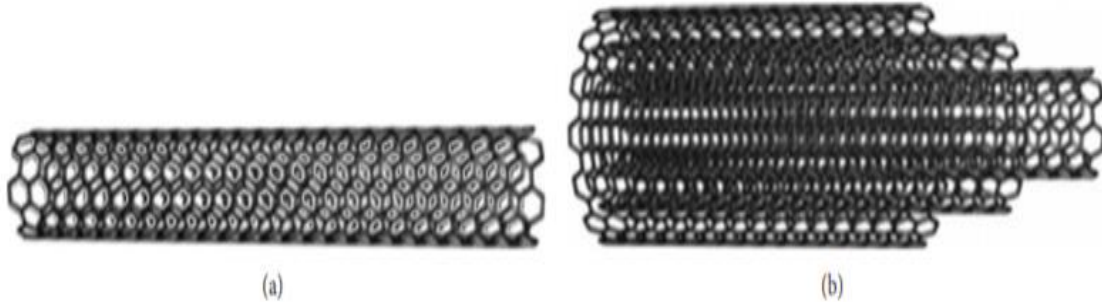
Graphene was originally observed in the year 1962 but was only studied while supported on metal surfaces. It was produced unknowingly in small quantities through the use of pencils and other applications of graphite. It was later rediscovered by Andre Geim and Konstantin Novoselov in 2004. Due to the availability of nanosize particles, it gave a new type of filler for multifunctional purposes. Graphene is one of the strongest and stiffest materials known to mankind. It also has a very high thermal conductivity of around $5000 \text{ Wm}^{-1}\text{k}^{-1}$. Graphene nanoplatelets have come across as one of the best nanofillers for composites which gives a balance between properties and cost.

1.2.5 Carbon nanotubes (CNTs)

(Andrews & Weisenberger, 2004) Carbon nanotubes (CNT) were discovered in 1991 by a Japanese physicist Sumio Iijima. CNT's have long tube-like structures with a diameter ranging from 2-10 nm and they can be hundreds to thousands of nanometers long. (Saifuddin et al., 2013) They are classified as Single-Walled Carbon Nanotubes (SWCNT) or Multi-Walled Carbon Nanotubes (MWCNT) based upon the number of graphene layers used to roll up the tube.

Figure 5

Carbon Nanotubes



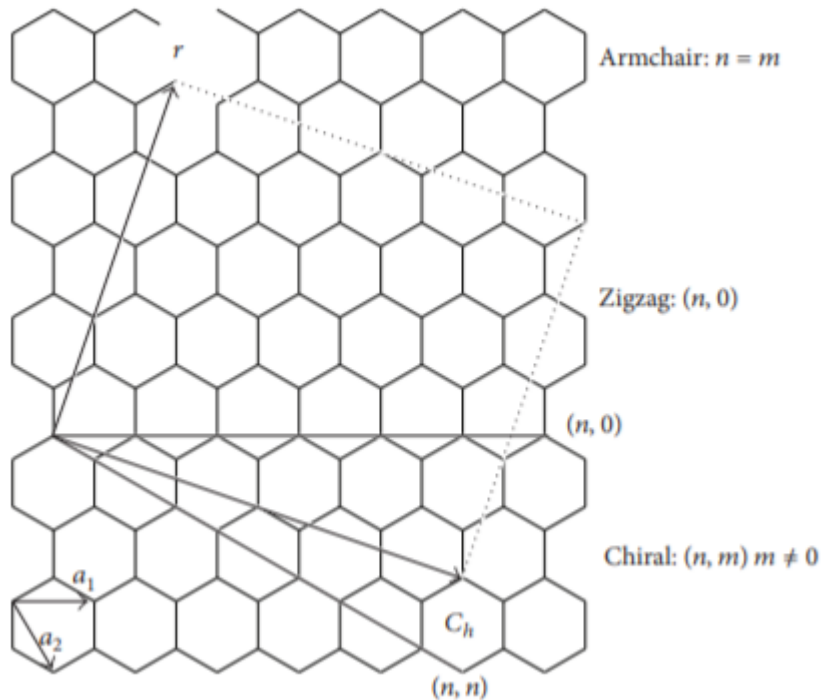
Note. 5(a) shows a Single-walled carbon nanotube. 5(b) shows a Multi-walled carbon nanotube. (Saifuddin et al., 2013)

In addition to the two basic structures, they are found in three different types based on how the graphene sheet is rolled up during its creation process. They are the Armchair, Zigzag, and Chiral. It depends on the values of n , m which are indices that represent the chiral vector where they correspond to the unit vectors along with the two directions in the honeycomb crystal lattice of graphene. When $n = m$, it is an 'armchair'

type CNT, when $m = 0$, it is called a ‘zigzag’ type CNT, and all other possibilities are known as ‘chiral’ type CNT.

Figure 6

Schematic Representation



Note. Schematic representation of the formation of carbon nanotube by rolling graphene sheet along lattice vectors to form chiral, armchair, and zigzag tubes. (Saifuddin et al., 2013)

CNT's can be manufactured using a variety of synthesis techniques in laboratory quantities. There are some challenges in preparing CNT's like Mass production i.e low cost, large scale, and high-quality CNTs, Selection production to control the structure and properties of CNTs, Organization to control the location and orientation of CNT on a flat substrate, and Mechanism to develop the understanding of nanotube growth. There are mainly three methods used to manufacture CNTs, arc discharge, laser ablation, and

chemical vapor deposition. All of the above-mentioned processes require a carbon source, high energy input, and catalyst. The principle of these three methods is the addition of high energy to a carbon source which results in fragments that recombine to form CNTs. In the case of the arc discharge method, the high energy source is electricity. For CVD, the energy source is heated from the furnace and a high-intensity light from a laser for the laser ablation method. The arc discharge and laser ablation method involves condensation of hot gaseous carbon atoms formed by evaporating the solid carbon source. But, due to the required equipment and energy expenses, these methods are not preferred over CVD for nanotube manufacturing. In CVD, the carbon nanotubes are produced at much lower temperatures of about 1200 °C. In this method, decomposition of a volatile carbon source takes place in the presence of a metallic catalyst which also acts as a site for carbon nanotube growth. The physical characteristics of the CNT can be well controlled using this method. Thus CVD method is used for large-scale productions of CNTs.

The properties and applications of CNTs have been well published over the years. (Spitalsky et al., 2010) Due to their highly unique thermal, electrical, and mechanical properties CNTs have been used as filler materials for polymer composite material. The elastic moduli of CNT range from 1.7 – 3.6 TPa. The tensile strength for MWCNT was found to be 11-63 GPa whereas the average breaking strength for SWCNT was up to 30 GPa. Apart from these mechanical properties, the electrical conductivity of individual MWCNT range from 10^7 - 10^8 S/m. The structural defects in CNTs lead to an increase in electric resistivity. (Hone et al., 2002) CNTs have also been reported to show extremely high values of thermal conductivity up to 6000 W/mK which makes them ideal as filler

material for polymer composites for thermal applications. They also have shown unique optical properties. To utilize the full potential of CNTs their composites are formulated. (Fabbro et al., 2012) Because of its wide area of applications, they are used in almost every field. CNTs can be used to treat breast cancer tumors by using them for targeted drug delivery systems. They are also used in aircraft and space applications because of their lightweight and high tensile strength. Similarly, they are used in manufacturing blades for windmills to produce electricity at a faster rate. CNTs can be used for filtrations purposes as they can filter out things having a diameter greater than that of CNT, they can be used to trap smaller size ions from a solution.

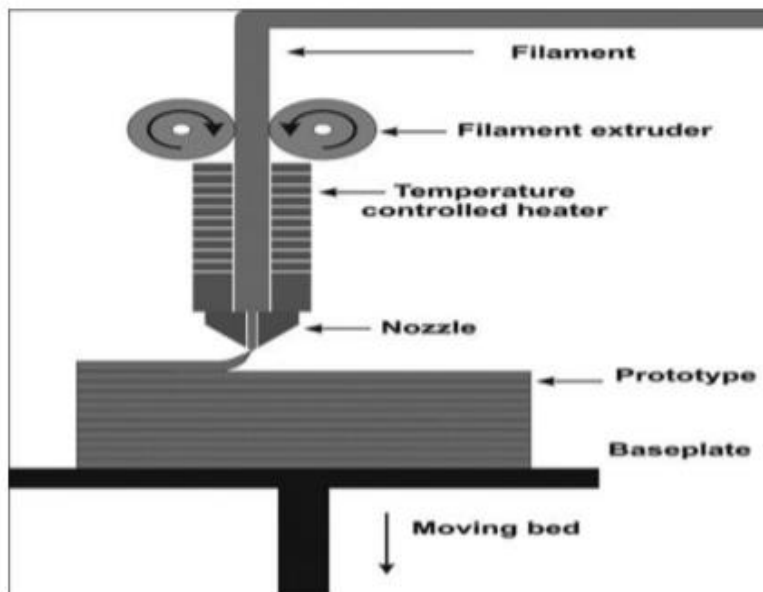
1.3 Additive Manufacturing Processes (AM)

Additive Manufacturing (AM) is a computer-controlled process that creates three-dimensional objects by depositing materials, usually layer by layer. AM can be categorized into seven types like vat photopolymerization, powder bed fusion, binder jetting, material jetting, sheet lamination, material extrusion, directed energy deposition, and hybrid. (Wohlers et al., n.d.) AM was first commercialized in the year 1987 by 3D Systems. They used SLA-1, which solidified thin layers of UV light-sensitive materials using a laser. In the year 1991, three other AM technologies were made commercially available, Fused Deposition Modeling (FDM) from Stratasys, Solid Ground Curing (SGC) from Cubital, and Laminated Object Manufacturing (LOM) from Helisys. Selective Laser Sintering (SLS) from DTM was made available in 1992.

1.3.1 Fused Depositing Modeling (FDM)

Figure 7

Fused Deposition Modeling (FDM)



Note. Schematic representation of FDM 3D printing. (Danayat et al., 2019)

Fused Deposition Modeling is also known as fused filament fabrication (FFF) and is one of the most common ways to 3D print polymer for rapid production purposes. (Bryll et al., n.d.) This technology was patented by Scott Crump, co-founder of Stratasys in 1989.

In this process, a thermoplastic filament is passed through a heated extruder head which deposits it on a built plate in XY direction. The temperature of the extruder head is higher than the melting point of the thermoplastic for ease of flow through the nozzle. If the temperature is not at an appropriate point then there might be issues like clogging of

the nozzles and print fails, etc. A contour is created of the object first and then it is filled with the material by a zigzag pattern of the head. The built plate lowers in the Z direction giving height to the object. This enables us to create complex geometries without many difficulties and additional processes that we might need for other traditional manufacturing processes. The FDM process starts with making a CAD model in software like Solidworks, AutoCAD, etc. After the model is prepared, it is incorporated in a program where process control parameters are defined as the temperature of the extruder and built plate, feed rate, layer thickness, supports, infill density, etc. Slicing of the model is done using slicing software to get each layer of the model. It is then stored in the machine which generates G codes for movement of the head according to each layer and thus a model is built. The finished built needs some post-manufacturing processes like removal of supports, polishing, and cleaning.

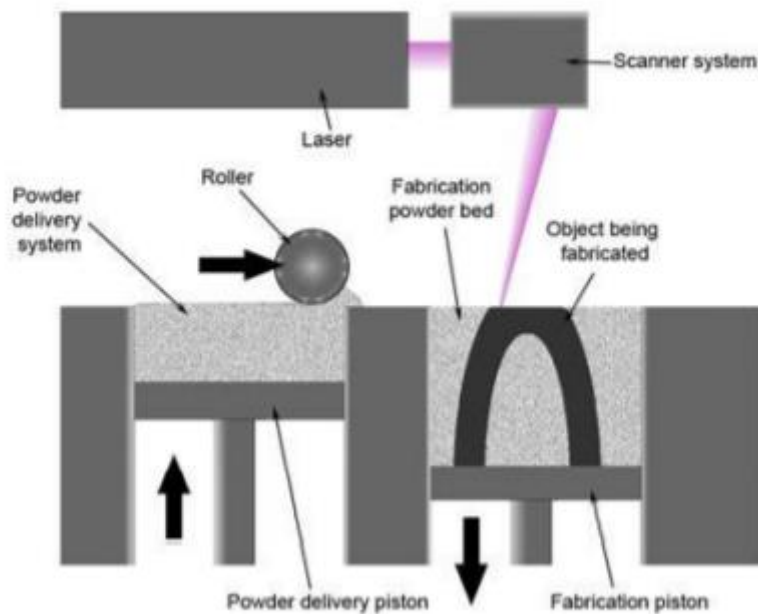
Some common defects can occur during FDM printing like shifted layers, burn marks, irregular walls, missing walls, overhang, warping, delamination, adhesion of layers, etc. There may be various causes for these defects which lead to print failures like human error, environmental causes like air draft and temperature, humidity, faulty design of model or wrong placement of supports, equipment malfunction, or else in some cases there might be an irregularity in the thermoplastic material.

1.3.2 Selective Laser Sintering (SLS)

Selective laser sintering (SLS) is a powder-based AM process. It was developed by Dr. Carl Deckard and Dr. Joe Beaman in the mid-1980s. They started the company DTM, later taken over by 3D Systems.

Figure 8

Selective Laser Sintering (SLS)



Note. Schematic representation of SLS 3D printing. (Danayat et al., 2019)

(X. Wang et al., n.d.) SLS process uses a high power laser to sinter the powder material together layer by layer. The use of high power laser makes home usage of the SLS method difficult due to safety and expense reasons. The laser selectively sinters powder by scanning the cross-sectional area across the powder bed in the XY direction of the model. After a layer is sintered, the powder bed lowers by one layer thickness in the Z direction and the same steps are repeated until a 3D model is formed. Some of the powder materials used in the SLS method are polyamides (PA), polystyrenes (PS), thermoplastic elastomers (TPE), and polyaryletherketones (PAEK) (*Selective Laser*

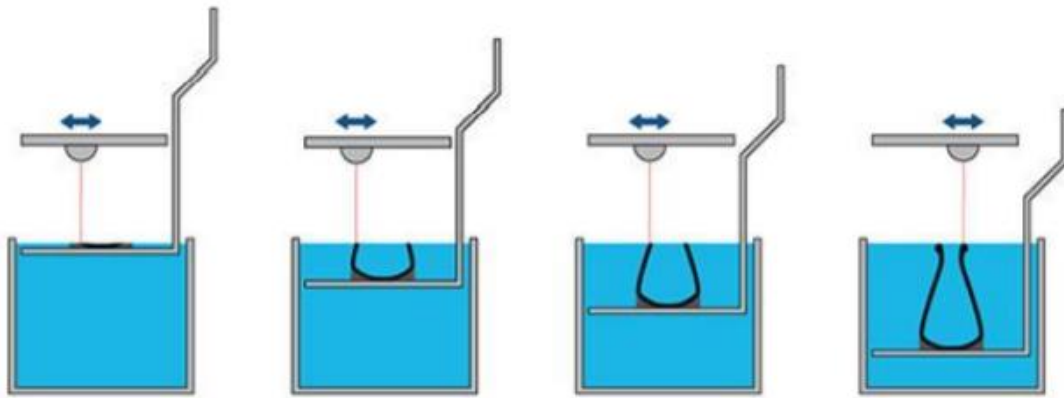
Sintering - Wikipedia, n.d.). The powder in the powder bed is heated to a temperature below the melting point to aid in the process of sintering with the use of a laser. Also, it is comparatively easy to print overhang structures as there are no supports needed as the unsintered powder in the bed acts as support. It is also possible to print multiple parts at a time by placing it at different places on the powder bed. Generally, cleaning of the part after printing is required. The use of a high-pressure air stream to blow off excess unsintered powder is one of the common methods. There are some limitations to SLS printing like hollow, completed closed structures that cannot be printed as there is no way to drain the excess powder from inside the part. The powder used in this method should be of high quality as it may hurt the properties of the part. If the powder is not closely packed in the powder bed it may lead to porosity in the structure of the part resulting in performance failure. The cost of the laser and other equipment with raw materials makes it a very expensive method of additive manufacturing. SLS is mainly used in industries for prototyping purposes in the design phase of a product life cycle and also for investment casting patterns, wind blades, automotive parts, etc

1.3.3 Stereolithography (SLA)

SLA stands for the stereolithography apparatus. It is a resin-based 3D printing process. In 1984, Chuck Hull patented the stereolithography process to create parts by printing thin layers in a succession of a photocurable medium by ultraviolet light.

Figure 9

Stereolithography (SLA)



Note. (Danayat et al., 2019)

(X. Wang et al., n.d.) Stereolithography uses a UV laser to cure photocurable resins. Nowadays DLP projector is also used as an inexpensive alternative to UV lasers. A pattern is projected in a vat containing the resin. A built platform is lowered in the vat tank. The UV laser/ DLP projector is focused on the built plate. The polymerization of the monomer resin takes place in the area of the projected pattern and a 2D layer is formed. Once the layer is formed, the built platform is lifted and the same process is repeated until a 3D object is formed. It is also possible to build parts in a bottom-up approach by using an inverted stereolithography machine (*Stereolithography - Wikipedia*, n.d.). The printed parts need to be washed with IPA to remove any excess uncured resin for safety reasons. Complex geometries can be easily printed using this process. Polymer

materials usually used as resins are epoxy, acrylic, etc. Photoinitiators or UV absorbers can be added to control the curing depth of the resin. Other factors that are critical for a successful print using the SLA process are the exposure time, lift speed of the built plate, down the speed of the built plate, delay, lift height. All these factors can help to minimize the defects in printing like delamination, adhesion, imperfect layers, etc. SLA printing is generally used to print parts with high resolutions. Also, since it is nozzle free, there are no issues of clogging as in the case of FDM printing. This process is fast, and parts printed using it has good mechanical properties and can be machined. Some of the disadvantages of SLA printing are that professional printing machines can be very expensive along with certain resin materials. Printed parts are required to be cured further after cleaning and drying.

CHAPTER 2

MATERIALS AND EXPERIMENTAL SETUP

2.1 Materials

2.1.1 Resin

Polyacrylate ester (Product name of Standard) having a viscosity of 146 cP, the dynamic viscosity of 250 cP, modulus of 1028 MPa, and tensile strength of 52 MPa was purchased from MakerJuice Labs in Kansas. The color of the resin was yellow. Due to the low viscosity of the resin, it does not need to be stirred while printing. The resin is sensitive from 365 nm to 420 nm wavelength light.

Figure 10

Pic of Resin in a Bottle and a Beaker



2.1.2 Carbon Nanotubes

Multi-walled carbon nanotubes(MWCNT) were bought from Cheaptubes. Inc (Grafton, VT). The outer diameter is 10-20 nm and its length is 10-30 μm with an average surface area of 233m²/g. The degree of purity of MWCNT was > 95% wt.

Figure 11

A TEM Image of MWCNTs



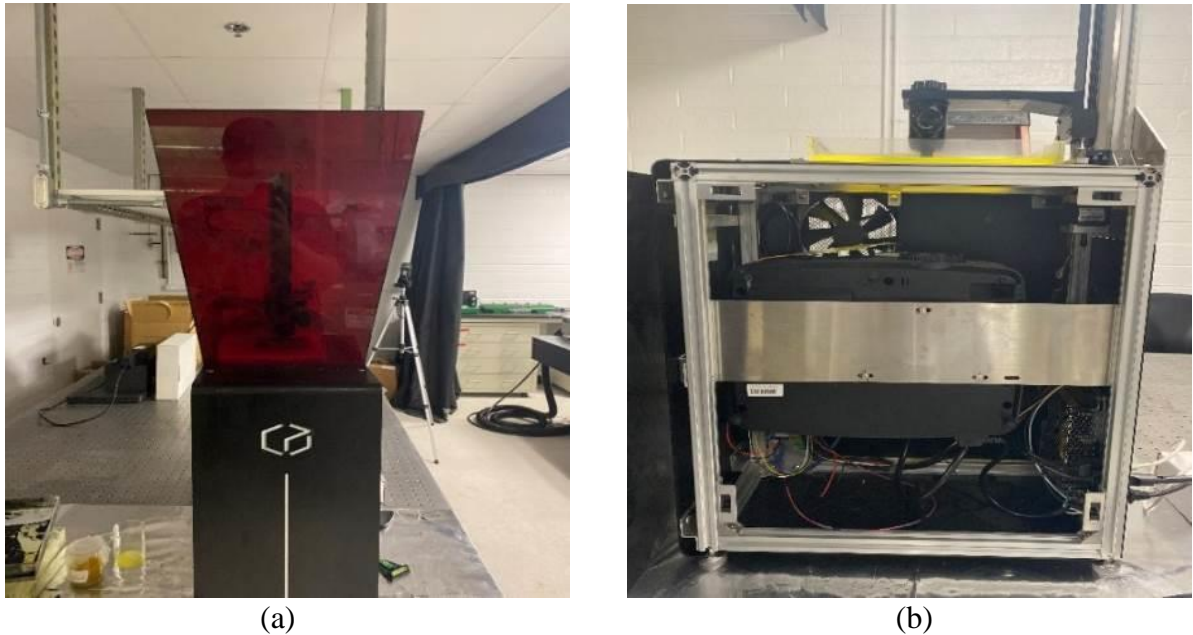
Note. (*Multi Walled Carbon Nanotubes 10-20nm / Cheap Tubes, n.d.*)

2.1.3 Titan 2

The 3D printer used for this study is TITAN 2 (Kudo 3D, Pleasanton, CA), with a built-in Raspberry Pi. The XY resolution of the printer is 23 μm – 26 μm . The maximum build height is 9.8 in. It has an HD DLP projector with a 2 cm native 1920 x 1080 DMD chip by Texas Instruments having a wavelength of 405 nm.

Figure 12

Setup for SLA 3D Printing



Note. Figure 12 (a) shows the front view of the SLA 3D printer (TITAN 2 Kudo 3D).

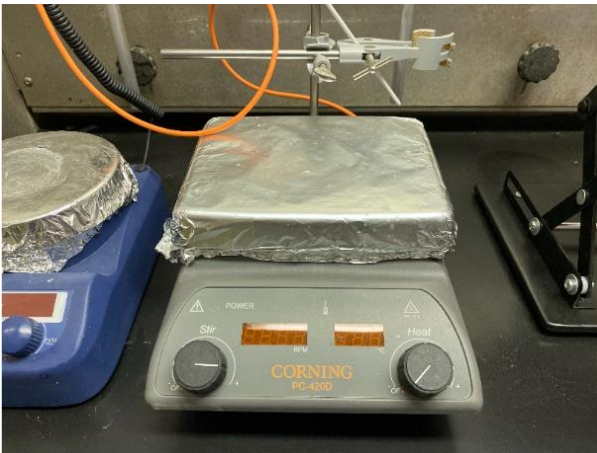
Figure 12 (b) shows the side view with an open panel to see the DLP projector.

2.2 Nanocomposite Preparation

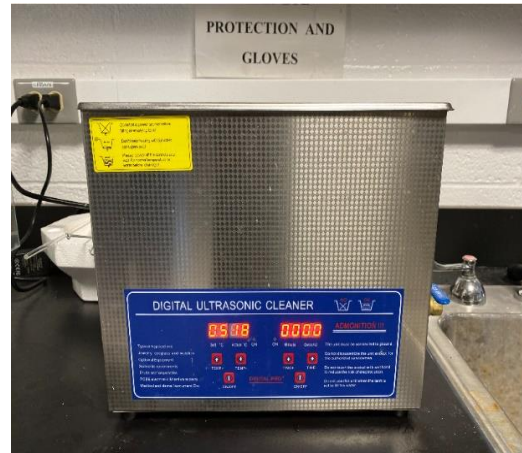
Before mixing the polymer and carbon nanotubes, they were measured to make composites with a wt ratio of 0.25%, 0.5%, and 1% of MWCNT. The samples with different concentrations of MWCNT were mixed thoroughly using a magnetic stirrer (Corning PC 240D) at 1050 rpm for 24 hrs. After mixing them using a magnetic stirrer, they were further mixed to make a homogenous mixture using the ultrasonication method. The samples were submerged in an ice bath during ultrasonication. The temperature was maintained at 10 °C. Each batch of the sample was ultrasonicated for 2-3 hrs.

Figure 13

Machines Used for Homogenous Mixing of Sample



(a)



(b)

Note. Figure 13 (a) is Corning PC 240D. Figure 13 (b) is a Digital Ultrasonic Cleaner

2.3 CAD Model and Parameter for 3D printing

In this thesis, for thermal testing, a simple cylindrical model was made using a designing software like SolidWorks 2019. The radius is 15 mm and the height (thickness) of the cylinder is 10 mm. The model is saved as a 3D-object in .stl format. This file is imported into ChiTubox V1.5.0 for slicing. The sliced file is saved in a .stl format and converted into a .csv format using a python program and then uploaded in the printer's software. In this study, the model is build using SLA 3D printing. The parameters for printing a sample with pure polymer are given in Table 3. The values of only exposure time change with different concentrations of MWCNT. For 0.25%, 0.5%, and 1% of MWCNT the value of exposure time is multiplied by the factor of 1.65, 2.57, and 5.15 respectively as shown in Table 4-6. These values were achieved by the trial and error method. Three samples for each concentration of MWCNT were made for testing

purposes. After the samples were printed the surfaces were polished using a sanding machine and cleaned using the IPA solution.

Table 3

Parameters for Printing Sample with Pure Resin

From Layer	To Layer	Exposure Time	Lift Height	Lift Speed	Down Speed	Delay time
1	1	35	40	15	150	1.2
2	10	20	40	15	150	1.2
11	20	12	40	15	150	1.2
21	40	10	10	15	150	1.2
41	199	10	10	15	150	1.2
200	400	5	10	15	150	1.2

Table 4

Parameters for Printing Sample with 0.25 wt% of MWCNT

From Layer	To Layer	Exposure Time	Lift Height	Lift Speed	Down Speed	Delay time
1	1	60	40	15	150	1.2
2	10	33	40	15	150	1.2
11	20	20	40	15	150	1.2
21	40	17	10	15	150	1.2
41	199	17	10	15	150	1.2
200	400	9	10	15	150	1.2

Table 5*Parameters for Printing Sample with 0.5 wt% of MWCNT*

From Layer	To Layer	Exposure Time	Lift Height	Lift Speed	Down Speed	Delay time
1	1	90	40	15	150	1.2
2	10	52	40	15	150	1.2
11	20	31	40	15	150	1.2
21	40	26	10	15	150	1.2
41	199	26	10	15	150	1.2
200	400	13	10	15	150	1.2

Table 6*Parameters for Printing Sample with 1 wt% of MWCNT*

From Layer	To Layer	Exposure Time	Lift Height	Lift Speed	Down Speed	Delay time
1	1	180	40	15	150	1.2
2	10	103	40	15	150	1.2
11	20	62	40	15	150	1.2
21	40	52	10	15	150	1.2
41	199	52	10	15	150	1.2
200	400	26	10	15	150	1.2

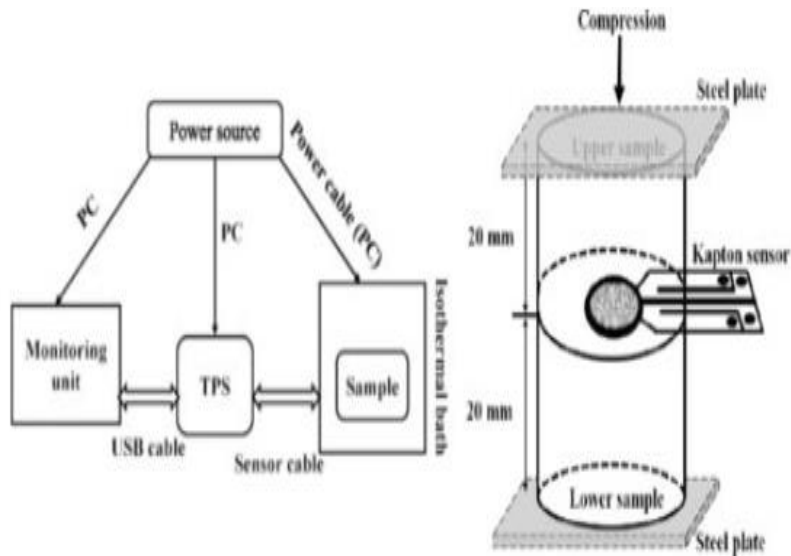
2.4 TPS 2500S

(Bouchard et al., 2013) The Hot Disk Technique is a transient plane source based on a disk sensor composed of a double spiral nickel wire for rapid thermal conductivity and diffusivity measurements. A Hot Disk TPS 2500S (Hot Disk AB, Gothenburg, Sweden) unit and a Kapton insulated sensor 5465 (radius 3.2 mm) were used to measure the thermal conductivity for the different concentrations of nanocomposites at room temperature according to ISO/CD 22007-2. This sensor is placed between two polished identical pieces with the same concentration of nanofillers in the nanocomposite samples (thickness of 10 mm and a radius of 15 mm) in a room-temperature sample holder represented in Figure 14 and 15. When a constant current is supplied to the sensor, it acts as a heat source and a temperature monitor. To validate a thermal conductivity measurement, different experimental specifications have been respected to minimize factors that could affect the results (especially contact resistance between the sensor and the material). All the samples' surfaces are made well smooth and parallel using a Diamond grade sanding paper on a UNIPOL-1210 sanding machine to minimize the surface irregularities. This enables optimal contact between the flat and thin TPS sensor and the polished samples, leading to a considerable reduction in contact thermal resistance between both elements. The samples were then cleaned with an IPA solution to remove any dust particles and limit their influence on the thermal conductivity measurement. Moreover, the hot disk method considers only data stemming from heat propagation in the materials for its calculations. The determined values, therefore, represent the bulk properties of the samples but must have to comply with other parameters. The probing depth i.e. the distance from the sensor edge to the nearest

surface of the sample must be smaller than 8 mm. Moreover, the temperature increase in the sensor must be over 0.4 C and the total to characterize time was fixed between 0.4 and 1 in the software parameters. For the accuracy issue, the mean deviation parameter was considered correct when it is below $1.103e^{-4}$. For each concentration of the nanocomposite, the heating power supplied by the sensor is fixed at 25 mW and 40 seconds. The associated change in temperature was recorded and an average of five thermal conductivity measurements per sample was collected.

Figure 14

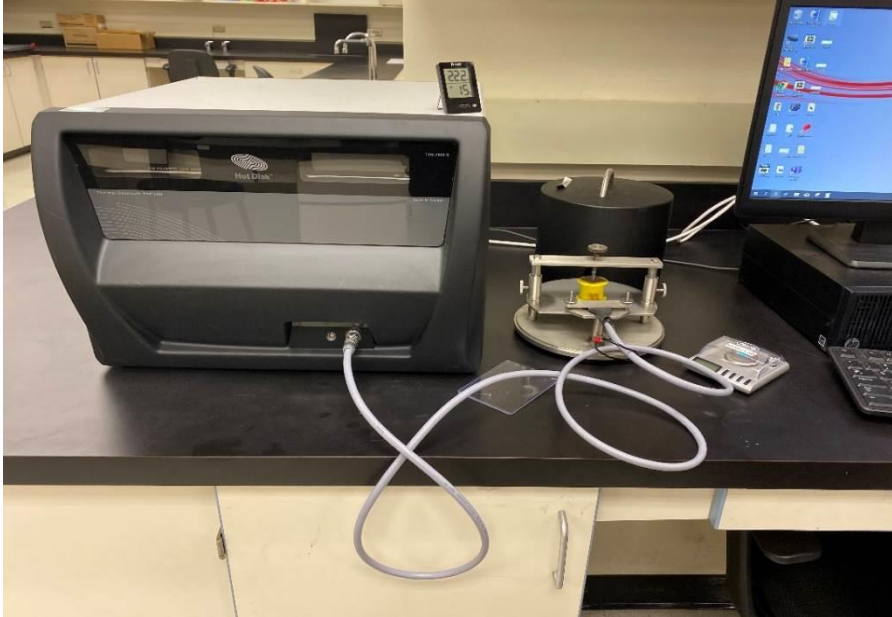
Schematic of TPS 2500S Test Arrangement



Note. (Rao et al., 2018)

Figure 15

Test Arrangement of TPS 2500S



CHAPTER 3

RESULTS AND DISCUSSION

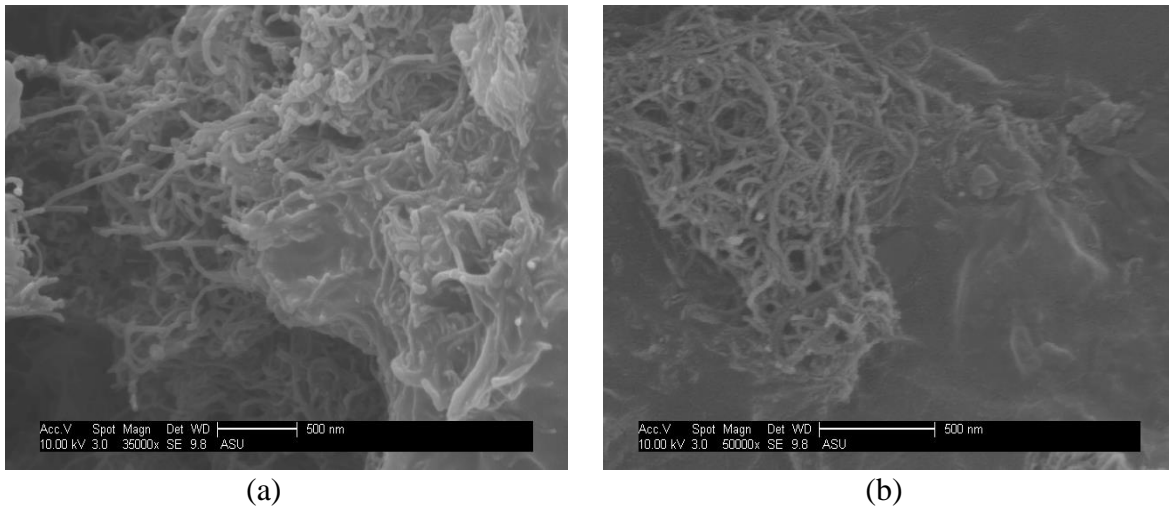
3.1 Dispersion of Filler Material

The state of dispersion of MWCNT in the polymer matrix greatly influence the thermal conductivity performance of the composite material. In a homogenous mixture, the formation of a CNT network increases the thermal conductivity of the material.

Therefore, to understand this concept, SEM images of all samples were studied.

Figure 16

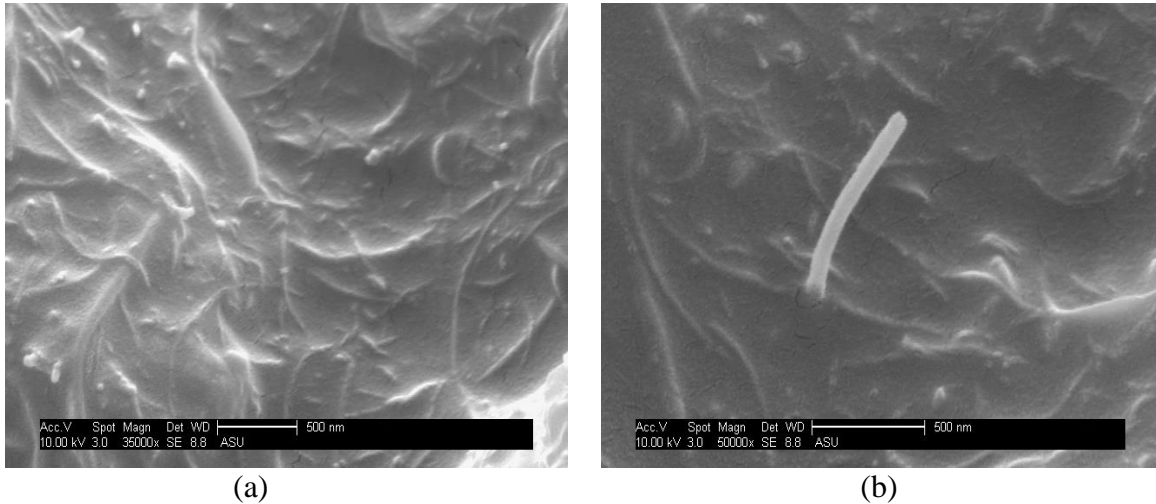
SEM Images of CNT Composite



Note. Figure 16 (a) shows SEM image of 0.25 wt% MWCNT composite. Figure (b) shows SEM image of 0.5 w% MWCNT composite.

Figure 17

SEM Images of CNT Composite



Note. Figure 17 (a) and (b) show SEM images of 1 wt% MWCNT composite.

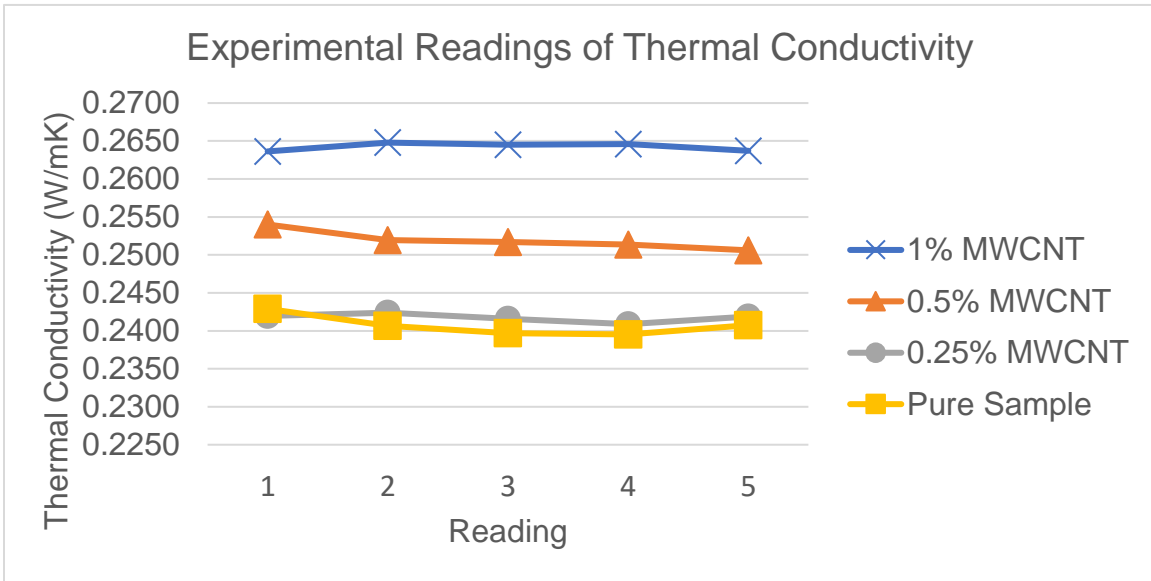
From Figure 16 (a) and (b) and Figure 17 (a) and (b), we can see that with the increase in the concentration of MWCNT, there is a denser thermal conductive network structure created. It is one of the contributing factors of the increase in the thermal conductivity of the MWCNT-polymer composite, which was further proved by carrying out an experimental thermal conductivity test with the help of TPS 2500S.

3.2 Measurement of Thermal Conductivity with Hot Disk 2500S

The testing was conducted at room temperature of 24⁰ C. For the measurement of thermal conductivity, five readings for each sample were taken at 25 mW for 40 sec each. Figure 18 shows the measured experimental values of thermal conductivity for each concentration.

Figure 18

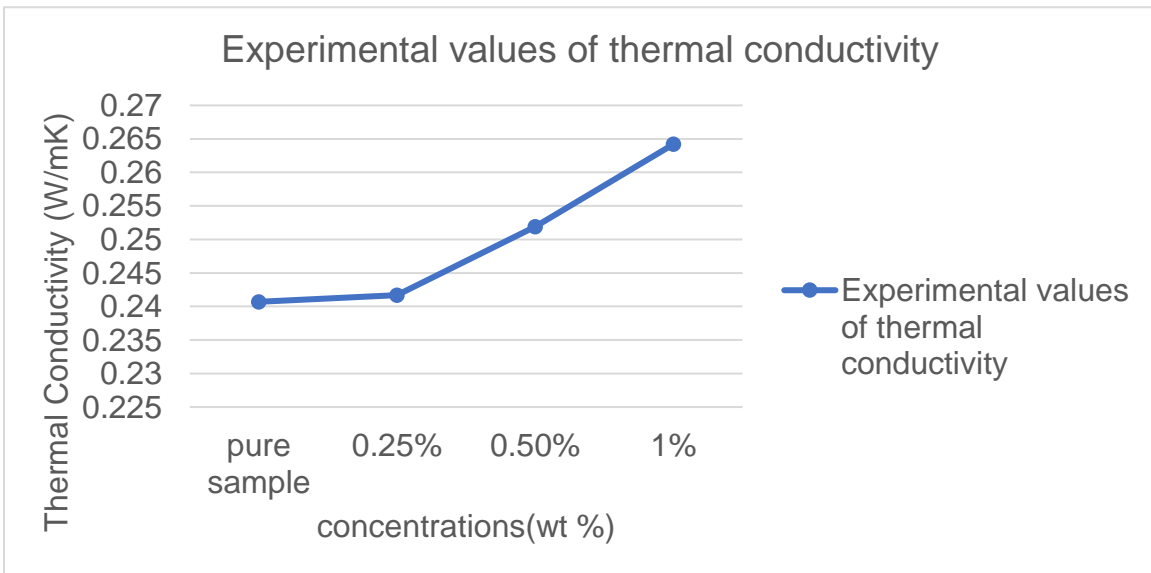
Experimental Readings of Thermal Conductivity



Note. Figure 18 shows 5 readings at different wt concentrations of MWCNT composites.

Figure 19

Experimental Values of Thermal Conductivity



Note. Figure 19 shows an increase in thermal conductivity with an increasing concentration of MWCNT in the composite material

The average value of the five readings for the thermal conductivity for pure polyacrylate ester is 0.2407 W/mK, which is close to the reported theoretical value of the material, which is 0.2 W/mK. With the increase in the concentration of just 0.25 wt% of MWCNT, there is no significant increase in the thermal conductivity of the composite material, as shown in Figure 19. By adding 0.5 wt% of MWCNT, the increase in thermal conductivity of the material is from 0.2407 W/mK to 0.2519 W/mK. At 1 wt% MWCNT content, the thermal conductivity of the composite material increases up to 0.2642 W/mK, which is a 9.76% increase than the pure sample. According to Figure 19, there is a gradual increase in the thermal conductivity of the composite material with an increasing concentration of multiwalled carbon nanotubes. This confirms the observations reported in the works of literature that the addition of MWCNTs facilitates the enhancement of the thermal conductivity.

3.3 Understanding thermal conductivity enhancement using different models

For a better understanding of the thermal conductivity of composite materials, several models have been proposed like Maxwell, Haminton – Crosser, Davis, Jeffery, Lu – Lin, Q.Z. Xue (Xue, 2005).

(Raja & Sunil, 2018) Maxwell and Haminton – Crosser models form the basis for many other derived models. All these models are developed to predict the effective thermal conductivity of composite material. Maxwell's model is based on Effective Medium Theory (EMT). This theory pertains to analytical or theoretical modeling that describes the macroscopic properties of composite materials (*Effective_medium_approximations @ En.Wikipedia.Org*, n.d.). There are certain assumptions made in Maxwell's model like there is low particle dispersion, the filler

particles a spherical, and the interactions between particles and base fluid temperature are neglected. Effective thermal conductivity by Maxwell’s model is given by the following equation.

$$\frac{k_e}{k_m} = 1 + \frac{3(\alpha-1)f}{(\alpha+2)-(\alpha-1)f} \dots\dots\dots(1)$$

where k_e is the effective thermal conductivity of the composite material, k_m is the thermal conductivity of the matrix, α is $\frac{k_c}{k_m}$, k_c is the thermal conductivity of filler material, f is the volume fraction of the filler material.

The Haminton and Crosser model is developed using the shape factor which takes into account both spherical and cylindrical particles. This model takes the structure and shape of the nanoparticles into consideration while calculating the effective thermal conductivity. The equation for Haminton – Crosser model is given by

$$\frac{k_e}{k_m} = \frac{\alpha+(n-1)-(n-1)(1-\alpha)f}{\alpha+(n-1)+(1-\alpha)f} \dots\dots\dots(2)$$

where n is given by $3/\psi$, and ψ is the ratio of the volume of the particle by the surface area of the particle. n is dependent upon the shape of the particle.

Jeffery’s model considers the interaction between the randomly dispersed nanoparticles in the matrix material. It can be used to calculate the effective thermal conductivities of composite materials containing only spherical particles. The equation is given by

$$\frac{k_e}{k_m} = 1 + 3\beta f + (3\beta^2 + \frac{3\beta^2}{4} + \frac{9\beta^3}{16} \frac{\alpha+2}{2\alpha+3} + \dots) f^2 \dots\dots\dots(3)$$

where β is $\frac{(\alpha-1)}{(\alpha+2)}$, the higher-order terms in Jeffery’s equation are due to the pair interactions between the randomly dispersed particles.

Davis's model is similar to Jeffery's model. Pair interactions of randomly orientated particles are taken into consideration in this model. The filler particles for this model are spherical. It is given by

$$\frac{k_e}{k_m} = 1 + \frac{3(\alpha-1)}{(\alpha+2)-(\alpha-1)f} [f + f(\alpha)f^2 + 0(f^3)] \dots \dots \dots (4)$$

(Lu & Lin, 1996) The Lu – Lin model for calculating the effective thermal conductivity of composite material is based on two models, which are the well-stirred model and the hard spheroidal model. In the well stirred and hard spheroidal models, a homogenous mixture for the composite material is required. It also takes into account a wide variety of inclusions like short fibers, needles, disks, and spheres. The equation for this model is represented by

$$\frac{k_e}{k_m} = 1 + af + bf^2 \dots \dots \dots (5)$$

where a and b are pure fitting parameters depending on the particles.

There are certain drawbacks to the above-mentioned models while calculating the effective thermal conductivity of the composite material. Firstly, the models are proposed for particles that are spherical or have small axial ratios and they do not consider the effect of space distribution of filler particles on the thermal conductivity of the composite material. As the filler material used for this research study are MWCNTs, which have a very large axial ratio, none of the above models can be used to evaluate the experimental results. The model used to compare the experimental results in this thesis is given by Q.Z. Xue.

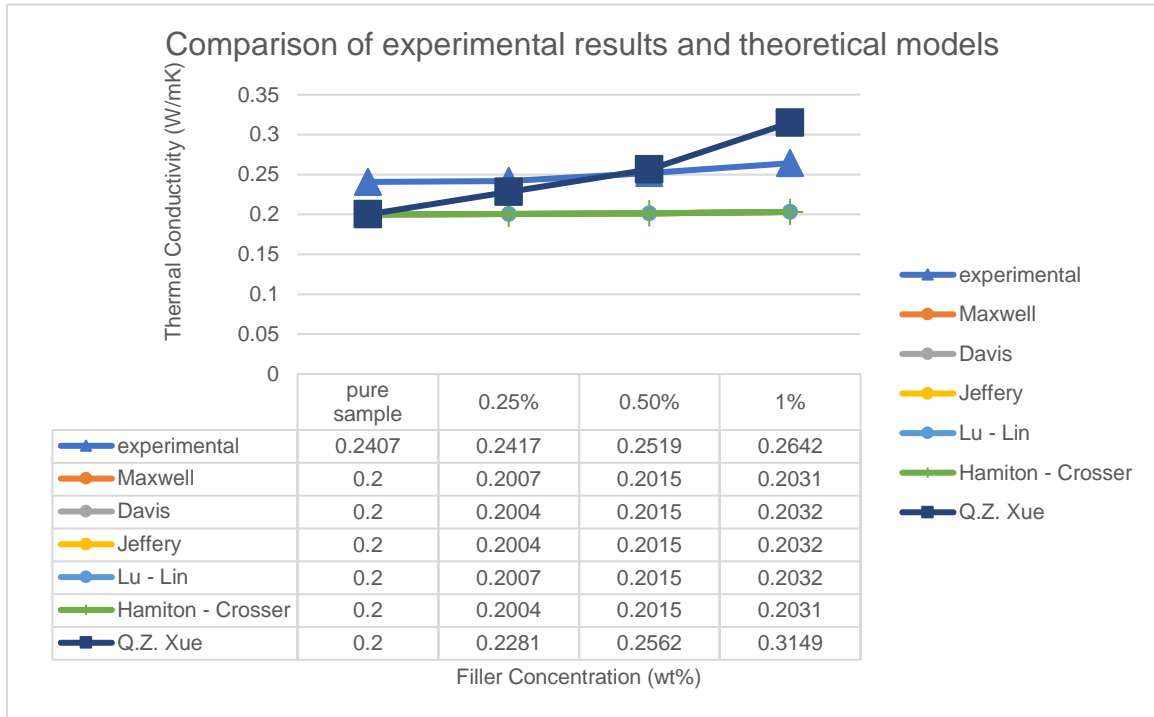
(Xue, 2005) The model proposed by Q.Z. Xue is based on the Maxwells model.

To take into consideration the shape of CNT particles Q.Z. Xue introduced a depolarization factor B_j and a distribution function $P(B_j)$ for the orientation distributing of CNTs in the polymer matrix. This overcomes the drawbacks of conventional models for the effective thermal conductivity of composite material. The equation for this model is given by

$$k_e = k_m \frac{1-f+\left(\frac{4f}{\pi}\right)\sqrt{k_c/k_m} \arctg(\pi/4\sqrt{k_c/k_m})}{1-f+\left(\frac{4f}{\pi}\right)\sqrt{k_m/k_c} \arctg(\pi/4\sqrt{k_c/k_m})} \dots\dots\dots(6)$$

Figure 20

Comparison of Experimental Results with Theoretical Models



Note. Figure 20 shows a comparison between the experimental test results with theoretical models for the thermal conductivity of different concentrations of composite material

Figure 20 shows the comparison of experimental results with the values from all the theoretical models. The value for k_m , k_c is taken as 0.20 W/mK and 600 W/mK respectively for calculation. For the Davis model $f(\alpha)$ is taken as 0.5. a , b for Lu – Lin model is taken as 3 and 4.51 respectively for MWCNT. n is taken as 3 for Haminton – Crosser model as ψ is 0.99999 which is equivalent to 1 for CNT.

We can see, that the values for the conventional model for the effective thermal conductivities are similar to one another. The relative increase in the thermal conductivity calculated using the conventional models for 1% wt concentration of MWCNT is 1.6% whereas, the relative increase for Q.Z. Xue model is 57.45%. The relative increase observed during the experimental thermal test shows an increase of 9.76% in the thermal conductivity of the composite material. Therefore, the experimental results lie within the boundaries of the conventional models and Q.Z. Xue model. If we could gather some more data points and increase the MWCNT concentration above the threshold value, it can be assumed that the experimental value may be in tandem with the values Q.Z. Xue model. It can be assumed that this is because of the Q.Z.Xue model considers the shape of CNT as well as the distribution of the filler particles while calculating the thermal conductivity of the composite materials. The difference between the theoretical values and the experimental value can be attributed to the inhomogeneous dispersion of filler material, agglomeration of CNT particles in the matrix, interface thermal resistance, etc.

(Zhang et al., 2015) To reduce the effect of interface thermal resistance, surface modification of CNT can be done. This leads to better interface thermal conductance between the polymer matrix and the filler material. By increasing the content of filler material agglomeration of CNTs can be tackled as at higher concentrations they will form

a network structure that indeed helps in better heat transport in polymer-based composites by conduction as this network provides a pathway for heat transport. The dispersion of CNT in the polymer matrix can be improved by adding materials that help in the dispersion of CNT by providing sites for contact.

CHAPTER 4

CONCLUSION

In conclusion, the main objective of this study was to study the fabrication of polymer-CNT nanocomposite material and the enhancement in its thermal properties. The polyacrylate – MWCNT composite is fabricated using SLA 3d printing method up to 1 wt% concentration.

An experimental test was carried out to measure the thermal conductivity of the composite material using TPS 2500S. Thermal conductivity results for 5 readings were recorded for an input of 25 mW for 40 sec. A 9.76 % increase in thermal conductivity is achieved in the polymer composite material. Different theoretical models were studied to verify the experimental test results. A comparison of thermal conductivity values for different models and the experiment data is shown in figure 20. It was observed that Q.Z. Xue model fits well with the data from the experimental study. The experimental values are similar to the predicted values. The reasons for the difference in the values for the theoretical model and experimental data are elaborated in chapter 3. The homogenous dispersion of filler material was studied using SEM images of samples.

CHAPTER 5

FUTURE SCOPE

Based on the observation of this study, further research needs to be done to improve the thermal properties of the polymer composite material. This chapter discusses some important areas in which further work needs to be done.

5.1 Higher filler Concentration

The sample concentration used in this study was not high enough. Using samples with an even higher concentration will lead to the formation of a network structure that will enhance the thermal conductivity of the composite material by providing an actual pathway on CNTs, as they tend to come in contact with adjacent CNT particles when in higher concentration.

One issue with using a higher concentration of CNT is that the viscosity of the composite material increases which results in difficulties during the printing process. Also, the exposure time required for curing layers of the composite material increases considerably.

5.2 Use of Different Material

Using a different polymer material as a matrix base can be a solution to reduce the increased viscosity of the composite material. Also, if the thermal conductivity is greater than the material being used, it can lead to an increase in the overall thermal conductivity. But, there are only a few polymers that can be printed using SLA 3d printing method. Therefore, we could use other methods to print the composite material, if it provides a variety of options for the polymer to be used along with increasing its thermal properties.

5.3 Surface Modification of Filler Material

Interfacial thermal resistance between the filler material and the polymer matrix leads to a loss in the thermal conductivity of the composite material. Appropriate surface modification can lead to a reduction in thermal resistance at the interface of polymer and filler material. (M. Wang et al., 2015) This can lead to an increase in thermal conductivity as shown in a study by Wang. Therefore, a further study in surface modification of CNT is required to reduce interfacial thermal resistance and increase the thermal conductivity of the composite material.

5.4 Incorporating in Thermal Applications

Lastly, the main objective of any research should be its incorporation in a real-world application. Therefore, further study should be made by using 3d printing techniques to print actual components/ parts using polymer composite material with MWCNT nanofillers for thermal applications like heat exchangers, heat sinks, water pipes, etc.

REFERENCES

- Andrews, R., & Weisenberger, M. C. (2004). Carbon nanotube polymer composites. *Current Opinion in Solid State and Materials Science*, 8(1), 31–37. <https://doi.org/10.1016/j.cossms.2003.10.006>
- Bouchard, J., Cayla, A., Devaux, E., & Campagne, C. (2013). Electrical and thermal conductivities of multiwalled carbon nanotubes-reinforced high performance polymer nanocomposites. *Composites Science and Technology*, 86, 177–184. <https://doi.org/10.1016/j.compscitech.2013.07.017>
- Bryll, K., Piesowicz, E., Szymański, P., Ślęczka, W., & Pijanowski, M. (n.d.). Polymer Composite Manufacturing by FDM 3D Printing Technology. *Matec-Conferences.Org*. <https://doi.org/10.1051/matecconf/201823702006>
- Danayat, S. S., Phelan, P., Kwon, B., & Azeredo, B. (2019). *Investigating 3-D Printed Polymer Heat Exchanger*.
Effective_medium_approximations @ en.wikipedia.org. (n.d.).
- Fabbro, C., Ali-Boucetta, H., Da Ros, T., Kostarelos, K., Bianco, A., & Prato, M. (2012). Targeting carbon nanotubes against cancer. *Chem. Commun*, 48, 3911–3926. <https://doi.org/10.1039/c2cc17995d>
- Fukushima, H. (2003). *GRAPHITE NANOREINFORCEMENTS IN POLYMER NANOCOMPOSITES*.
fullerene nanofiller - Google Search. (n.d.). Retrieved September 12, 2020, from https://www.google.com/search?q=fullerene+nanofiller&tbm=isch&ved=2ahUKEwiK0uPTtOTrAhWTmJ4KHWDWakEQ2-cCegQIABAA&oq=fullere&gs_lcp=CgNpbWcQARgAMgQIIxAnMgQIIxAnMgIADICCAyAggAMgIADICCAyAggAMgIADICCAA6BQgAELEDUMLiL1jP7i9gnv4vaABwAHgAgAFjiAHqBJIBATeYAQCgA
- graphene nanoplatelets - Google Search*. (n.d.). Retrieved September 12, 2020, from https://www.google.com/search?q=graphene+nanoplatelets&tbm=isch&ved=2ahUKEwiCs_m1ueTrAhVBhJ4KHe2IB2oQ2-cCegQIABAA&oq=gr&gs_lcp=CgNpbWcQARgBMgQIIxAnMgQIIxAnMgQIAB BDMgQIAB BDMgQIAB BDMgQIAB BDMgQIAB BDMgQIAB BDMgUIABCxAzIFCAAQsQM6AggAUKL6Clj-wpg04oLaABwAHgAgAFx
- graphite nanopowder - Google Search*. (n.d.). Retrieved September 12, 2020, from https://www.google.com/search?q=graphite+nanopowder&tbm=isch&ved=2ahUKEwjgp5LLt-TrAhUJAjQIHx7A_AQ2-cCegQIABAA&oq=gr&gs_lcp=CgNpbWcQARgBMgQIIxAnMgQIIxAnMgQIAB BDMgQIAB BDMgQIAB BDMgQIAB BDMgUIABCxAzIFCAAQsQM6AggAUKL6Clj-wpg04oLaABwAHgAgAFx
- Hone, J., Llaguno, M. C., Biercuk, M. J., Johnson, A. T., Batlogg, B., Benes, Z., & Fischer, J. E. (2002). Thermal properties of carbon nanotubes and nanotube-based materials. *Appl. Phys. A*, 74(3), 339–343. <https://doi.org/10.1007/s003390201277>

- Lu, S. Y., & Lin, H. C. (1996). Effective conductivity of composites containing aligned spheroidal inclusions of finite conductivity. *Journal of Applied Physics*, 79(9), 6761–6769. <https://doi.org/10.1063/1.361498>
- Multi Walled Carbon Nanotubes 10-20nm / Cheap Tubes*. (n.d.). Retrieved September 12, 2020, from <https://www.cheaptubes.com/product/multi-walled-carbon-nanotubes-10-20nm/>
- nanocomposites, S. T.-R. advances in polymer, & 2009, undefined. (n.d.). Polymer-graphite nanocomposites. *Books.Google.Com*. Retrieved September 13, 2020, from [https://books.google.com/books?hl=en&lr=&id=o2HvBQAAQBAJ&oi=fnd&pg=PA19&dq=Tjong,+S..+\(2009\).+Polymer-Graphite+nanocomposites.+&ots=SuAYR4Y6x_&sig=vGiXydP37yv7A9_9kUWsl_kf2IE](https://books.google.com/books?hl=en&lr=&id=o2HvBQAAQBAJ&oi=fnd&pg=PA19&dq=Tjong,+S..+(2009).+Polymer-Graphite+nanocomposites.+&ots=SuAYR4Y6x_&sig=vGiXydP37yv7A9_9kUWsl_kf2IE)
- Nanodiamonds add some sparkle to imaging | Research | Chemistry World*. (n.d.). Retrieved September 12, 2020, from <https://www.chemistryworld.com/news/nanodiamonds-add-some-sparkle-to-imaging/7847.article>
- Penkova, A. V., Acquah, S. F., Piotrovskiy, L. B., Markelov, D. A., Semisalova, A. S., & Kroto, H. W. (2017). Fullerene derivatives as nano-additives in polymer composites. *Russian Chemical Reviews*, 86(6), 530–566. <https://doi.org/10.1070/rcr4712>
- Raja, R. A. A., & Sunil, J. (2018). Estimation of Thermal Conductivity of Nanofluids Using Theoretical Correlations. In *International Journal of Applied Engineering Research* (Vol. 13, Issue 10). <http://www.ripublication.com>
- Rao, C. R. C., Niyas, H., & Muthukumar, P. (2018). Performance tests on lab–scale sensible heat storage prototypes. *Applied Thermal Engineering*. <https://doi.org/10.1016/j.applthermaleng.2017.10.085>
- Saifuddin, N., Raziah, A. Z., & Junizah, A. R. (2013). Carbon nanotubes: A review on structure and their interaction with proteins. *Journal of Chemistry*, 2013. <https://doi.org/10.1155/2013/676815>
- Santos, A., & Martel, E. (2018). Recent Progress in Biomedical Applications of Nanodiamonds. *Nanoscience and Nanotechnology*, 8(1), 11–24. <https://doi.org/10.5923/j.nn.20180801.03>
- Selective laser sintering - Wikipedia*. (n.d.). Retrieved September 14, 2020, from https://en.wikipedia.org/wiki/Selective_laser_sintering
- Spitalsky, Z., Tasis, D., Papagelis, K., & Galiotis, C. (2010). Carbon nanotube-polymer composites: Chemistry, processing, mechanical and electrical properties. In *Progress in Polymer Science (Oxford)* (Vol. 35, Issue 3, pp. 357–401). <https://doi.org/10.1016/j.progpolymsci.2009.09.003>
- Stereolithography - Wikipedia*. (n.d.). Retrieved September 14, 2020, from <https://en.wikipedia.org/wiki/Stereolithography>
- Verma, R., Song, K., Jiang, H., & Nian, Q. (2018). *Design, Fabrication and Characterization of PVA/Nanocarbon Composite Fibers*.

- Wang, M., Hu, N., Zhou, L., & Yan, C. (2015). Enhanced interfacial thermal transport across graphene-polymer interfaces by grafting polymer chains. *Carbon*, 85, 414–421. <https://doi.org/10.1016/j.carbon.2015.01.009>
- Wang, X., Jiang, M., Zhou, Z., Gou, J., Engineering, D. H.-C. P. B., & 2017, undefined. (n.d.). 3D printing of polymer matrix composites: A review and prospective. *Elsevier*. Retrieved September 14, 2020, from <https://www.sciencedirect.com/science/article/pii/S1359836816321230>
- Wohlers, T., report, T. G.-W., & 2014, undefined. (n.d.). History of additive manufacturing. *Wohlersassociates.Com*. Retrieved September 14, 2020, from <http://www.wohlersassociates.com/history2016.pdf>
- Xue, Q. Z. (2005). Model for thermal conductivity of carbon nanotube-based composites. *Physica B: Condensed Matter*, 368(1–4), 302–307. <https://doi.org/10.1016/j.physb.2005.07.024>
- Yadav, J. (2018). Fullerene: Properties, Synthesis and Application. *Research & Reviews: Journal of Physics*, 6(3), 1–6. <https://doi.org/10.37591/RRJOPHY.V6I3.68>
- Zhang, W. Bin, Zhang, Z. X., Yang, J. H., Huang, T., Zhang, N., Zheng, X. T., Wang, Y., & Zhou, Z. W. (2015). Largely enhanced thermal conductivity of poly(vinylidene fluoride)/carbon nanotube composites achieved by adding graphene oxide. *Carbon*, 90, 242–254. <https://doi.org/10.1016/j.carbon.2015.04.040>
- Zuev, V. V. (2011). Polymer Nanocomposites Containing Fullerene C60 Nanofillers. *Macromolecular Symposia*, 301(1), 157–161. <https://doi.org/10.1002/masy.201150320>